

# Simple Design for Singlemode High Power CW Fiber Laser using Multimode High NA Fiber

Bertrand Morasse\*, Stéphane Chatigny, Cynthia Desrosiers, Éric Gagnon, Marc-André Lapointe, Jean-Philippe de Sandro,  
CorActive High-Tech, 2700 Jean-Perrin, suite 121, Québec, Canada, G2C 1S9

## ABSTRACT

A large number of high power CW fiber lasers described in the literature use large mode area (LMA) double cladding fibers. These fibers have large core and low core numerical aperture (NA) to limit the number of supported modes and are typically operated under coiling to eliminate higher order modes. We describe here multimode (MM) high NA ytterbium doped fibers used in single mode output high power laser/amplifier configuration. Efficient single mode amplification is realized in the multimode doped fiber by matching the fundamental mode of the doped fiber to the LP<sub>01</sub> mode of the fiber Bragg grating (FBG) and by selecting the upper V-number value that limits the overlap of the LP<sub>01</sub> to the higher order modes. We show that negligible mode coupling is realized in the doped fiber, which ensures a stable power output over external perturbation without the use of tapers. Fundamental mode operation is maintained at all time without coiling through the use of FBG written in a single mode fiber. We show that such fiber is inherently more photosensitive and easier to splice than LMA fiber. We demonstrate an efficient 75W singlemode CW fiber laser using this configuration and predict that the power scaling to the kW level can be achieved, the design being more practical and resistant to photodarkening compared to conventional low NA LMA fiber.

**Keywords:** High power CW fiber laser, multimode fiber, single mode operation, splicing, mode matching, high numerical aperture fiber, fiber Bragg grating

## 1. INTRODUCTION

High power CW laser sources with hundreds of watts up to several kilowatts are required for different industrial application such as material processing. Silica based fiber laser and amplifier are of great interest for their excellent beam quality, large heat dissipation, high power handling and robustness, which give significant advantages over traditional gas or crystal based lasers. Especially, ytterbium (Yb) doped fiber amplifier is used for its high efficiency, high doping concentration, and large pump absorption band. Furthermore, double-cladding optical fiber (DCOF) configuration allows a large amount of low brightness high power pump source to be coupled into a large fiber cladding and amplify a high brightness signal to high power in a small core with high beam quality. Up to 6 kW singlemode ytterbium fiber laser was recently demonstrated using such principle<sup>[1]</sup>.

Excellent beam quality close to the limit of diffraction is often sought to improve the focus properties of the beam. Double-cladding fiber laser with singlemode core can easily maintain a fundamental beam mode. But scaling at higher power requires typically larger core to limit non-linear effects<sup>[2]</sup> and maintain acceptable pump absorption from the larger cladding required to accommodate more pump power. Then one of the challenges of fiber laser is to design and operate them with a diffraction limited beam quality at high power. One popular approach to achieve it is to use large mode area (LMA) designs where a few moded low NA large core is operated in the fundamental mode. For instance, 700 W of output power was demonstrated in a 20 μm core diameter with 0.06 NA<sup>[3]</sup> and 1.36 kW with a 43 μm/0.05NA core<sup>[4]</sup>. In such configuration, high order modes (HOM) are further suppressed using coiling that induces higher loss to the HOM compared to the fundamental mode<sup>[5]</sup>. Micro-structure fibers<sup>[6]</sup> can be used in a similar way to reach the kW level with high beam quality from their enlarged fundamental mode area design. Tapers<sup>[7]</sup> and mode field adaptor<sup>[8]</sup> (MFA) were also used to improve the beam quality of high power CW fiber laser by properly selecting the fundamental mode. Singlemode excitation of multimode fibers was also used to get a high beam quality output specifically for an amplifier configuration<sup>[9],[10]</sup>.

In this work we describe a simple design to obtain single mode high power CW fiber laser using multimode (MM) high NA fiber without the use of tapers or MFA. We use the principle of singlemode excitation of MM fibers<sup>[9],[10]</sup>, but

\*bertrand.morasse@coractive.com; phone: 1 (418) 845-2466; fax: 1 (418) 845-2609; www.coractive.com

Copyright 2009 Society of Photo-Optical Instrumentation Engineers.

This paper is published in Proceeding of SPIE (Photonics West 2009) and is made available as an electronic reprint (preprint) with permission of SPIE. One print or electronic copy may be made for personal use only. Systematic or multiple reproduction, distribution to multiple locations via electronic or other means, duplication of any material in this paper for a fee or for commercial purposes, or modification of the content of the paper are prohibited.

applying it to CW fiber laser in a robust all-fiber monolithic configuration easy to integrate. We first introduce the motivations of high NA MM fiber design such as the large working tolerance, the high power scalability, the photodarkening mitigation and 960 nm pumping with phosphorous codoping. Then the theoretical analysis of modes excitation and coupling in MM fiber is presented. And finally experimental validations of the design are demonstrated.

## 2. MOTIVATIONS OF MULTIMODE HIGH NA FIBER DESIGN

As previously introduced, one can use many ways of achieving high power Yb singlemode CW fiber laser and using multimode design is one option. But the motivations and advantages of using high NA multimode fiber are better understood when comparing it to LMA designs mostly reported in the literature. We describe in this section a selected MM high NA configuration and its advantages compared to LMA based configuration in term of MFD stability, scalability to the kW level, photodarkening and pumping scheme.

### 2.1 Selected configuration

A configuration using high NA multimode fiber to get high power CW output is shown on Figure 1. Any fiber laser design is highly dependent upon the pump source and the combiner technology used, which will affect the number of pump branches at each injection point, the cladding diameter of the fiber, the number of amplifier stages, etc. In this paper we will keep our focus on the fiber design, especially the core parameters. Then the core design can be adapted to the required pumping scheme by choosing the appropriate cladding diameter.

The configuration shown below is a master-oscillator-power-amplifier (MOPA) scheme. The master oscillator (MO), also known as the seed, is a Fabry-Perot oscillator with Fiber Bragg Gratings (FBG) of high (HR) and low reflectivity (LR) that determines the emission wavelength. For instance a 99.9 % HR of 3 nm bandwidth centered at 1075 nm can be used with a 10% LR of 1 nm bandwidth at 1075 nm. It can be judicious to choose a HR's bandwidth greater than the LR's to compensate for potential thermal drift of the FBG. Pumps diodes are coupled to the MO using a combiner having  $N$  pump branches coupled to a common output port ( $N \rightarrow 1$ ). The FBG are made strictly in singlemode fiber at 1075 nm to ensure a fundamental mode oscillation while the Yb gain fiber is a high NA multimode fiber with a high V-number (see equation 1).

A MO alone might not reach the desired output power level due to pump power limitations, so a power amplifier (PA) can be cascaded to further amplify the signal from the MO. Pump sources are coupled in the PA with a pump combiner coupling  $N$  pump branches and one signal branches into a common output port ( $N+1 \rightarrow 1$ ). In order to mitigate non-linear effects at higher power, the PA's gain fiber is a high NA multimode fiber but with a larger mode field diameter (MFD). The fundamental mode operation of the PA is insured by pigtailing it to singlemode undoped fibers at 1075 nm. These details will be discussed in more details later in the paper, but as an example, the MO is made of  $10\mu\text{m}/0.20\text{NA}$  Yb fiber with  $6\mu\text{m}/0.12\text{NA}$  relay fiber and the PA with  $15\mu\text{m}/0.13\text{NA}$  Yb fiber with  $8\mu\text{m}/0.10\text{NA}$ . The signal feed through of the PA combiner is made of a  $7\mu\text{m}/0.11\text{NA}$  fiber to optimize the matching between the MO and the PA without using MFA.

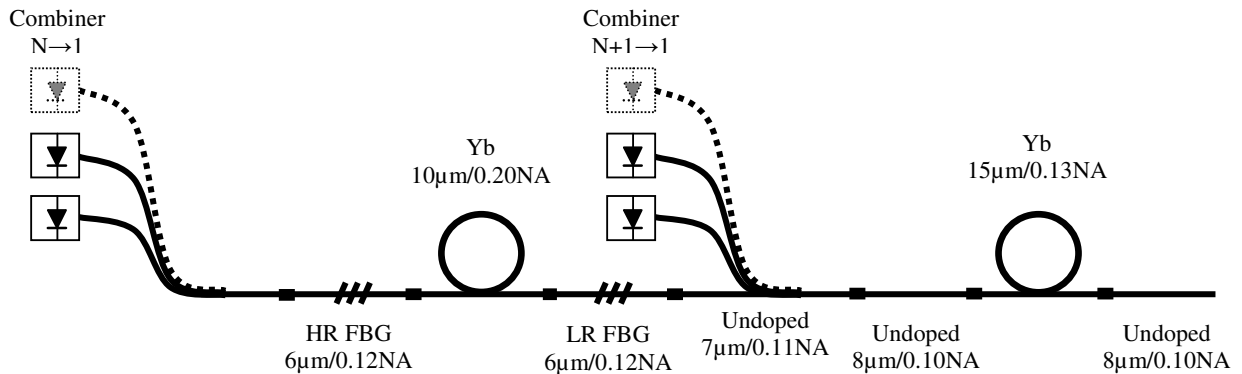


Figure 1. An example of proposed MOPA configuration for high power CW fiber laser showing the core diameter/core NA for all the components used: high and low reflectivity (HR and LR) fiber Bragg gratings (FBG), the ytterbium (Yb) doped fiber and the undoped delivery fiber.

In another hand, a typical LMA configuration would use low NA fiber such as  $10\mu\text{m}/0.08\text{NA}$  for the MO with  $10\mu\text{m}/0.08\text{NA}$  FBG pigtailed. The power amplifier would be a  $20\mu\text{m}/0.065\text{NA}$  fiber with a large cladding coiled to suppress higher order modes. The delivery fiber would be a  $20\mu\text{m}/0.065\text{NA}$  with a MFA between the two stages to connect the  $10\mu\text{m}/0.08\text{NA}$  to the  $20\mu\text{m}/0.065\text{NA}$ .

## 2.2 Large tolerances of high NA fiber

The use of highly NA MM fibers exhibit several advantages. First of all, high NA MM fiber allows a larger tolerance on the refractive index profile while maintaining a stable modal behavior and easy spliceability. Using equations 1 and 2 presented in section 3.1, the MFD variation with respect to the refractive index variation can be calculated. The results are presented on Figure 2 for the LMA fiber and the high NA MM fiber introduced in the configuration above. It is clear that the high NA fiber has a much higher MFD stability than the LMA design. This gives a much more stable splicing process over a large number of cavities which is important for production purposes. The advantage of higher NA versus low NA design was also presented by Sévigny and al.<sup>[11]</sup>.

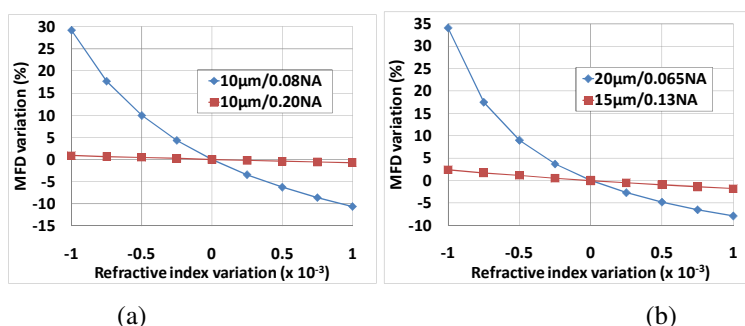


Figure 2. MFD variation as a function of the refractive index variation of the core for a MM high NA design versus a LMA design for (a) the master oscillator and (b) the power amplifier fibers shown in the configuration of Figure 1. The results clearly show that the MFD is less sensitive to refractive index variation in high NA MM fibers.

Furthermore, the use of LMA fiber requires a photosensitive core in low NA fiber to allow FBG photo-inscription for Fabry-Perot CW laser cavity. A minimum amount of photosensitive element such as germanium is required for UV photo-inscription (typically more than 1.5 mol% of germanium oxide). It is then required to use another index-lowering element such as fluorine or boron to preserve a low NA below 0.08. As such elements are very volatile and have different glass transition temperature, the splicing process and NA matching are then much more difficult and less repeatable.

## 2.3 High power scalability of small core

LMA fibers are mostly used to increase the mode field area and limit non-linear effects, especially stimulated Raman scattering (SRS) that dominates in large linewidth CW high power fiber laser. However, the SRS threshold is often overestimated in fiber laser design and the kW level can be reached in much smaller core diameter. Simple analytical formulae exist to calculate SRS as presented by Agrawal<sup>[11]</sup>; however, some assumptions need to be made for the effective length since amplification occurs and also some residual gain of the Yb in the 1100-1150 nm range can influence the Raman effect. The operation of a kilowatt class laser in order to measure the Raman threshold is difficult and costly to conduct in the laboratory mainly because of the amount of required pump power, the design of all the fibers and combiners with different core/cladding configurations. A simple experiment can be conducted to accurately determine the SRS threshold of high power CW fiber laser using low power pulsed amplifiers. Square pulses of 50 ns pulsewidth and 200 kHz repetition rate can be produced by a seed diode at 1064 nm and pre-amplified to 200 mW average power. The pulses are then amplified in an Yb fiber at average power in the range of 1 to 10 W, which is equivalent to peak power of 100 W to 1 kW. The output spectrum is then monitored to detect the apparition of SRS. Care was taken to make sure there is no intra-pulse CW signal and no signal in the fiber cladding. An Yb pump absorption of 0.55 dB/m at 915 nm with a length of 25 m were used to conduct the amplifier test, which is equivalent to typical length of fiber used in high power CW fiber laser to minimize thermal effect. An aluminosilicate fiber with  $6\mu\text{m}/0.12\text{NA}$  core and two phosphosilicate fibers with  $7\mu\text{m}/0.19\text{NA}$  and  $8\mu\text{m}/0.10\text{NA}$  cores were all tested in that setup and gave consistent threshold results. The 200 kHz repetition rate was selected such that the output pulse energy was

below the saturation energy level of the fibers and does not bring pulse deformation<sup>[12]</sup>, which gives accurate output peak power calculation. Results for the 6 $\mu$ m/0.12NA fiber are shown on Figure 3.

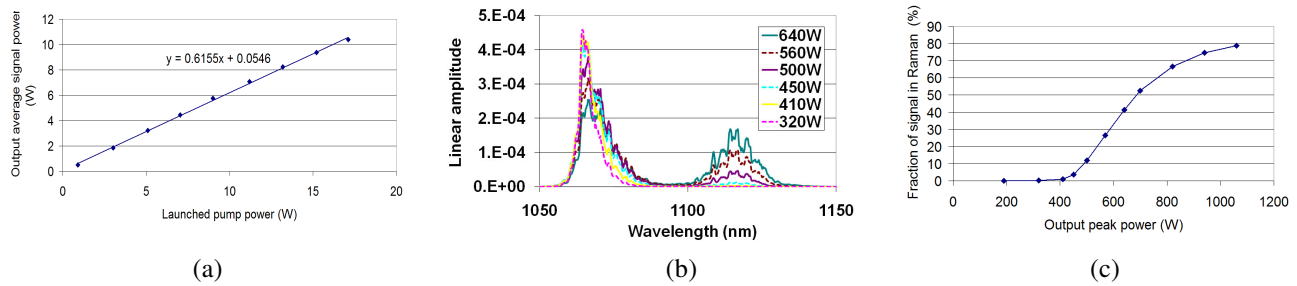


Figure 3. Pulsed amplifier tests done at 50ns/200kHz in 25m of double cladding 6 $\mu$ m/0.12NA aluminosilicate fiber with 0.55 dB/m of absorption to evaluate the Raman threshold of a CW fiber laser: (a) average output power as a function of launched pump power, (b) output spectrum at different output peak power and (c) fraction of signal in Raman wavelength as a function of output peak power. The 1% Raman threshold is thus evaluated at 408 W output power for a 7 $\mu$ m MFD.

The SRS threshold can clearly be seen on the output spectrum. Any power lost to Raman wavelength will be useless in many applications so we define the SRS threshold at the level where 1% of signal power is transferred to the first Raman stoke. For the 6 $\mu$ m/0.12NA fiber, this threshold corresponds to 408 W output peak power. The mode field diameter (MFD) of the ytterbium fiber was measured at 1064 nm with an EXFO's NR9200 and found to be 7.0  $\mu$ m, which corresponds to the calculated value from equation (2) in section 3.1 below. The same experiment was done with the 7 $\mu$ m/0.19NA phosphosilicate fiber and the SRS threshold was found to be 307 W for a MFD of 6.0  $\mu$ m. So the ratio of the SRS threshold over the mode area was found to be very similar for an aluminosilicate and a phosphosilicate fiber. Similar SRS threshold of mode area was determined with the 8 $\mu$ m/0.10NA phosphosilicate fiber.

The SRS is known to be directly proportional to the mode area<sup>[1]</sup>, so a direct extrapolation can predict that the kilowatt level would be reached with a 11  $\mu$ m MFD fiber. So LMA designs such as 20 $\mu$ m/0.065NA are way over-kill to reach the kW level since the MFD is in the order of 16  $\mu$ m typically. High NA MM design with lower MFD are thus sufficient to achieve most fiber laser with 100's of watts of output power and a kW fiber laser could be done with a 15 $\mu$ m/0.13NA MM fiber for instance which has a MFD of 11.5  $\mu$ m as presented in the configuration of Figure 1.

#### 2.4 Photodarkening mitigation with high NA fiber and 960 nm pumping

Photodarkening is known to be problematic in ytterbium doped fiber<sup>[13],[14]</sup>. This phenomenon is known as an increase in optical losses occurring in the fiber core which results in a decrease of output power over time. Photodarkening can be mitigated in some way by codoping with aluminum but it can be dramatically reduced by codoping with phosphorous<sup>[15],[16],[17]</sup>. Codoping with phosphorous is also known to stabilize photodarkening much faster for stable long term operation compared to aluminum codoping<sup>[18]</sup>. For instance, we conducted a 1047 nm core pump darkening test, which gives similar inversion level than cladding pumping, over a 10 m long of singlemode aluminosilicate fiber over 4000 hours and found no stabilization in the temporal power loss as shown on Figure 4. So even if aluminum codoping can allow only a very small photodegradation of a few percent over 1000 hours in a given configuration, it is very likely that this degradation will continuously run and becomes significant over 10 000 or 20 000 hours operation. Though aluminum codoping combined with fluorine or boron codoped fiber can mitigate photodarkening in a certain extent in low NA LMA design, a high NA design with phosphorous co-doping allow a very stable output power over thousands of hours of operation reached by traditional laser such as crystal based laser.

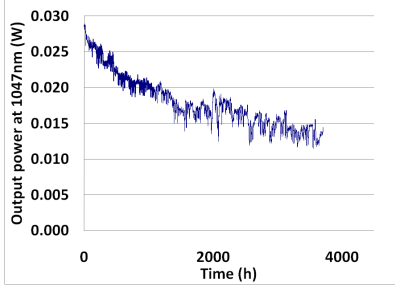


Figure 4. Photodarkening test with 200 mW of core pumping power at 1047 nm of a singlemode aluminosilicate fiber over several thousands of hours.

Furthermore, the use of phosphosilicate fibers gives a flat absorption spectrum from 910 nm to 970 nm that allow an efficient pumping in that range compared to aluminosilicate fiber that will have low absorption outside the 915 nm band. The main advantage of pumping for instance at 965 nm with a phosphosilicate fiber instead of 915 nm with an aluminosilicate fiber is that the quantum defect will be smaller with respect of the emission wavelength around 1075 nm. Typically 5% more output power is obtained with a pump wavelength difference of 50 nm which reduces the thermal load of the active fiber as well. We do not consider here the 975 nm absorption band because fine wavelength tuning is typically required for most pump sources due to the narrow linewidth of this absorption band for both phosphosilicate and aluminosilicate fibers.

### 3. THEORETICAL ANALYSIS

In this section, the theoretical analysis of the singlemode operation of high NA multimode fiber is presented. The singlemode operation rely on optimizing the mode matching of the fundamental mode of the singlemode relay fiber with the MM high NA Yb fiber while minimizing the excitation and coupling to higher order modes in the MM fiber. The fundamental mode matching will be described in a simple manner using the step index approximation in section 3.1 and also in a more general and complete manner using a radially stratified model that simulate arbitrary refractive index profile in section 3.2. Higher order modes excitation and coupling will be described in section 3.3 and 3.4 respectively.

#### 3.1 Fundamental mode matching using step index approximation

In order to obtain a stable singlemode operation of multimode fiber, we need to insure a perfect and controlled fundamental mode excitation of the Yb high NA MM fiber. The light is launched from a strictly singlemode fiber and collected by the same fiber. Thus, a very good mode matching between the fundamental modes of the single mode fiber and the MM high NA Yb fiber is required. The step index approximation can accurately model the singlemode operation of high NA MM fiber with analytical equations. The model is explained in different textbook<sup>[19],[20]</sup> and the main useful equations are summarized below. It considers a simple step index fiber of core diameter  $D$  and refractive index difference  $dN$ . The refractive index difference is more often given in term of numerical aperture ( $NA$ ). From the  $NA$  and core diameter  $D$ , the normalized frequency  $V$ , also called V-number, can be calculated at a given operation wavelength  $\lambda$ . The equation of  $NA$  and V-number are then given by the following:

$$NA = \sqrt{(n_{silice} + dN)^2 - n_{silice}^2} \quad V = \frac{\pi \cdot NA \cdot D}{\lambda} \quad (1)$$

The fiber supports only the fundamental mode when  $V < 2.405$ . The higher the V-number above the value of 2.405, the larger are the number of higher order modes propagated into the fiber. The fundamental normalized intensity mode profile  $I(r)$  propagating into the fiber can be approximated using a Gaussian profile or radius  $w$ . Typically, the mode field radius represents the radius at 13.5% ( $1/e^2$ ) of the maximum intensity profile. The coupling efficiency  $\eta$  between two fibers of mode field radii  $w_1$  and  $w_2$  can then be calculated with a simple formula. The mode profile  $I(r)$ , the mode field radius  $w$ , and the coupling efficiency  $\eta$  can then be approximated with the following equations:

$$I(r) = \exp\left(-\frac{r^2}{w^2}\right) \quad w = \frac{D}{2} \left(0.65 + \frac{1.619}{V^{3/2}} + \frac{2.879}{V^6}\right) \quad \eta = \left(\frac{2w_1w_2}{w_1^2 + w_2^2}\right)^2 \quad (2)$$

Therefore, the coupling efficiency of the fundamental mode of any fiber with a given core diameter  $D$  and numerical aperture  $NA$  (or  $dN$ ) can be analytically calculated using equations 1 and 2. For instance, if a master oscillator is composed of FBG written in a  $6\mu\text{m}/0.12NA$  singlemode fiber as described on Figure 1, the proper high NA MM Yb matching fiber must be found with appropriate core diameter and NA. A typical calculation is shown on Figure 5 where the coupling efficiency of the  $6\mu\text{m}/0.12NA$  fiber with the MM fiber is plotted as a function of the core diameter of the MM fiber for three NA values of 0.16, 0.18, and 0.20. The results show that a core diameter of  $9\mu\text{m}$  gives the optimum coupling efficiency between the fundamental mode of the SM fiber and the MM fiber regardless of the NA of the MM fiber.

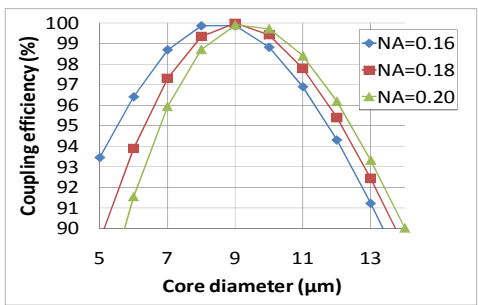


Figure 5. Coupling efficiency between a  $6\mu\text{m}/0.12NA$  singlemode fiber and a high NA MM fiber as a function of the core diameter and the NA of the MM fiber. An optimum core diameter of  $9\mu\text{m}$  is found regardless of the NA value.

### 3.2 Fundamental mode matching using radially stratified model

Most fibers do not have a perfect step index profile and it is worth modeling the mode field distribution with a more accurate model that can take into account an arbitrary refractive index profile. To do this, we used a radially stratified representation of the fiber refractive index profile (RIP)<sup>[21]</sup>. The refractive index profile is subdivided into a finite number of slices and the supported modes are found by solving the wave equation using a transfer matrix formalism.

For instance, we want to design a high NA MM fiber such that its fundamental mode perfectly matches the one of a  $10\mu\text{m}/0.08NA$  singlemode (SM) fiber. The exact refractive index profile can be measured on the fiber itself using the refracted near field method with an EXFO’s NR9200 (using TIA/EIA-455-44B (FOTP-44B) “Refractive Index Profile, Refracted Ray Method”). The refractive index profile of the MM fiber could be measured on the preform directly before drawing, but to avoid any measurement calibration between different apparatus, a small section of the MM fiber is drawn and the RIP is measured as well on the NR9200. Such measurement result is shown on Figure 6-(a) for a given MM fiber along with the selected  $10\mu\text{m}/0.08NA$ .

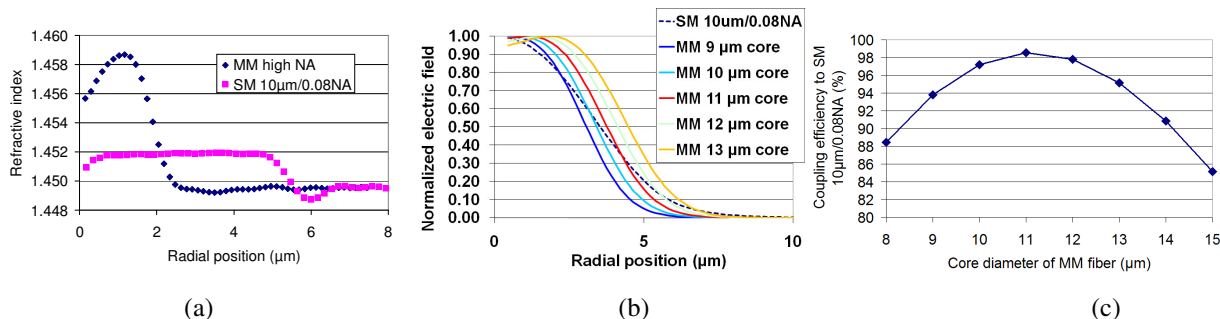


Figure 6. (a) Measured refractive index profile of a MM high NA fiber and a SM  $10\mu\text{m}/0.08NA$ . (b) Simulated mode field profile of the SM  $10\mu\text{m}/0.08NA$  and the MM fiber for various targeted core diameter of the MM fiber. (c) Coupling efficiency between the  $10\mu\text{m}/0.08NA$  singlemode fiber and the high NA MM as a function of the core diameter of the high NA MM fiber. An optimum core diameter of  $11\mu\text{m}$  is found for the high NA MM fiber which gives a coupling efficiency of 98% with the SM fiber.

Using the measured refractive profile, the mode field profile can be simulated and coupling efficiency can be calculated by doing the overlap integral between the two modes<sup>[20]</sup>. Since the refractive index profile is preserved regardless of the targeted core diameter, the MM fiber can be drawn with the optimum radius such that the coupling efficiency with the

10 $\mu\text{m}$ /0.08NA is maximized. The resulting calculation is shown on Figure 6-(b) and (c). Nevertheless, it is worth noting that the splicing can degrade or improve the predicted coupling coefficient because of dopant diffusion.

Even though the radially stratified model allows to simulating any arbitrary refractive index profile, we noted that the step index approximation gives interesting results close to the experimental results when the centerline dip is not too pronounced in the refractive index profile. So the simple analytical equations remain interesting and useful.

### 3.3 Higher order modes excitation

Even if a perfect match occurs between the fundamental mode of the SM fiber and the MM fiber, higher order modes can still be excited in the MM fiber if a given overlap exists. The fundamental mode has especially a good overlap with LP<sub>0X</sub> even modes, which have a circular symmetry like the LP<sub>01</sub> mode. The mode intensity profile of the LP<sub>0X</sub> modes supported by an 11 $\mu\text{m}$ /0.22NA are shown on Figure 7-(a), which are the LP<sub>01</sub>, LP<sub>02</sub>, and LP<sub>03</sub>. We can calculate with the overlap integral<sup>[20]</sup> that the coupling efficiency between the fundamental mode is around 3 % with the LP<sub>02</sub> and 1 % with the LP<sub>03</sub>.

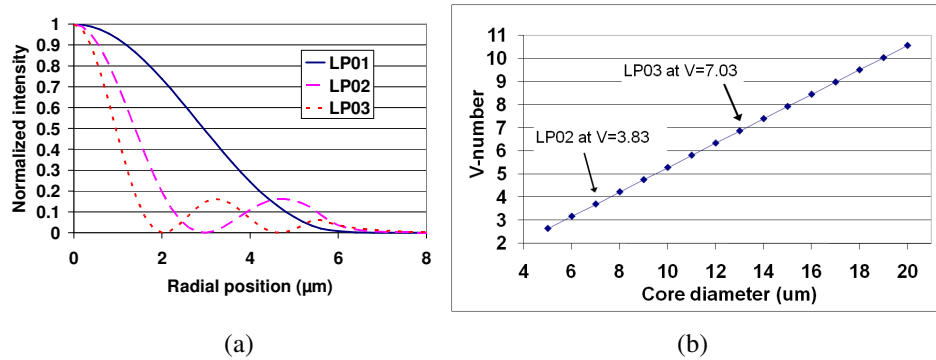


Figure 7. (a) Normalized intensity profiles of the even modes LP<sub>01</sub>, LP<sub>02</sub>, and LP<sub>03</sub> of a 11 $\mu\text{m}$ /0.22NA fiber. The overlap between the LP<sub>01</sub> and the higher order even modes LP<sub>02</sub> and LP<sub>03</sub> are 3% and 1% respectively. (b) V-number of a 0.18 NA MM fiber as a function of its core diameter. The cut-off of the LP<sub>02</sub> and LP<sub>03</sub> modes occur at a core diameter of 8  $\mu\text{m}$  and 13  $\mu\text{m}$  respectively.

Therefore it is important to consider and optimize the HOM content of the high NA MM fiber being used and specially avoid LP<sub>0X</sub> HOM excitations. The V-number can clearly indicate the number of supported modes of a step index fiber. Taking for instance a 0.18 NA MM fiber, the V-number at 1070 nm is plotted as a function of the core diameter on Figure 7-(b) using equation (1). Knowing that the LP<sub>02</sub> and LP<sub>03</sub> mode will occur at V-number of 3.83 and 7.03 respectively, which correspond to a core diameter of 8  $\mu\text{m}$  and 13  $\mu\text{m}$ , the appropriate core diameter can be drawn from this information. If a low power fiber laser is required, a 7  $\mu\text{m}$  core size can be selected, minimizing the excitation of all higher order LP<sub>0X</sub> modes. But if a higher output power is required, a 12.5  $\mu\text{m}$  core diameter is appropriate: the bigger core will limit non-linear effects but the trade-off is that a few percents of power will be transferred to HOM. This analysis is important because it can be noted that for the last case, it is worthless to go at core diameters ranging from 8  $\mu\text{m}$  to 12  $\mu\text{m}$  because the excitation of HOM will not be significantly lower and using a smaller core decreases the pump absorption significantly. Higher doping level to compensate a smaller core cannot be achieved easily because of photodarkening effect and control of background losses. The same conclusions can be drawn for the case of a low power fiber laser with a 7  $\mu\text{m}$  core where going to smaller core diameter is not advantageous. The same exercise can be done with a more complete model such as the radially stratified model and similar analysis and conclusions can be found compared to the step index approximation.

It can be noted once again that this overlap calculation is done by considering a perfect butt coupling, but in practice, the fibers are spliced and the modes can be perturbed from small misalignment, angular offset, and refractive index modification at the splice point. Thus, a coupling to higher order modes can be expected to occur in a somewhat different amount than simulated, especially with low NA fiber smaller than 0.10 NA that are very sensitive to MFD variation.

### 3.4 Higher order modes coupling

Even if the fundamental mode is primarily excited at the launching point, coupling to higher order modes is possible during light propagation. The closer the effective indexes of the modes are, the more likely they will interact and power

from the fundamental modes will be transferred to higher order modes<sup>[22]</sup>. Then, one advantage of high NA multimode fibers is that the mode separation is much larger than LMA fiber. For instance, taking two fibers with the same V-number, a LMA 20 $\mu\text{m}/0.07\text{NA}$  and a high NA MM 9 $\mu\text{m}/0.16\text{NA}$ , the mode separation between each mode is three times larger in the high NA MM fiber than in the LMA fiber as shown on Figure 8. Therefore the high NA MM fiber will be much more resistant to higher order mode coupling<sup>[22]</sup>: once the fundamental mode is excited, the power will remain in that mode. We experimentally observed in the experiments reported below that a high NA MM fiber amplifier or laser is very resistant to external perturbation: the singlemode efficiency is strictly unchanged even if the ytterbium fiber or the splice points are coiled to very small radii smaller than 2 cm or if strong external pressure is applied on the fibers. Therefore, high NA MM designs are very robust over external perturbations and are easy to package for industrial applications.

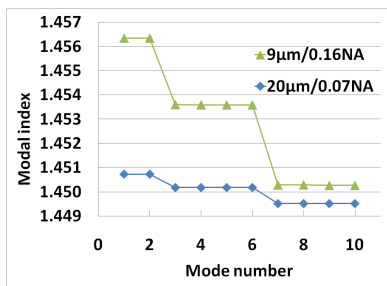


Figure 8. Effective modal indexes of a LMA 20 $\mu\text{m}/0.07\text{NA}$  compared to a high NA MM 9 $\mu\text{m}/0.16\text{NA}$  fiber showing that a high NA MM fiber has a greater mode separation.

## 4. EXPERIMENTS

### 4.1 Splice optimization

To optimize the singlemode operation of MM high NA fibers, the splice process must be considered properly. A setup like the one shown on Figure 9 can be used to do such optimization for the case of a CW fiber laser cavity or in a very similar fashion for amplifier. A light source outside the absorption band of the ytterbium (800 to 1200 nm) ions, such as 1310 nm diode, is used in order to monitoring the splice losses. It is still possible to use a source in the absorption band to optimize the splice for optimum SM operation, but then the exact splice loss value cannot be measured. A broadband source with small coherence length such as a light emitting diode (LED) is preferred to avoid spectral interferences that can give fluctuations in the power measurement. The light source must also have power stability in the range of 0.05 dB since the splice loss can be in that order of magnitude; the fiber optics power meter must also be accurate and repeatable in the same power range. We typically use an Hewlett Packard broadband light source 83437A and an ILX power meter FPM-8210H to do such measurement. Since the high and low reflectivity fiber Bragg gratings (HR and LR FBG) are made in double cladding optical fiber, cladding mode strippers (CMS) must be done on these fiber to properly measure the power transmission in the core. Any power propagating in the cladding will still be detected at the power meter and falsify the splice loss measurement. So the CMS ensures that the injected light and measured light are in the core of the fiber. To do so, 15 cm of fiber is uncoated and high index epoxy is applied directly onto the silica cladding over all the uncoated length. Some curvatures can be added to the fiber to improve the CMS. Another way to strip the cladding modes is to simply put a few meters of single cladding fiber before and after the two FBGs used since light is attenuated in the high index of the single cladding fiber. It is also important to collect the power at the output with a singlemode fiber since to make sure the power loss of the fundamental mode is measured.

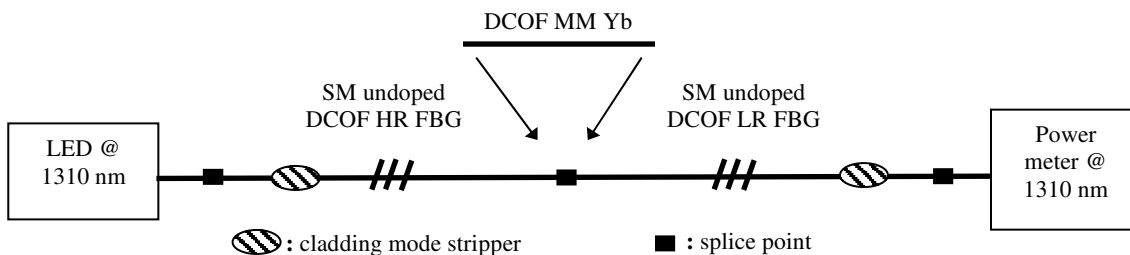


Figure 9. Setup to measure and optimize the fundamental mode transmission in the Yb MM high NA fiber.



The first step is to splice together the two FBGs and take a reference power  $P_{ref}$  in dBm. Then the splice is cut and the Yb fiber is spliced in between the two FBGs and the output power  $P_2$  is measured in dBm. Considering an ytterbium fiber of length  $L$  in meters and of background loss at  $BL$  in dB/m at the measurement wavelength, the splice loss  $Sp$  for one splice is given by equation (3). The measurement setup gives the splice loss value of two splices, so a factor of one half is added in equation (3) to give the loss value of each splice.

$$Sp = \frac{1}{2} (P_2 - P_{ref} - BL \cdot L) \quad [\text{dB}] \quad (3)$$

The first splice optimization that can be done is to manually align the cores of the fibers when splicing, also called active alignment. In practice, the core of the fiber are not perfectly centered with respect to the cladding due to manufacturing tolerances of optical fiber, so any core offset increases the splice loss or excites higher order modes. Typical splicers available on the market have the option of manually aligning the fibers. The best way to do it is to first quickly splice the ytterbium between the FBG using a rough cladding alignment and then redo each splice with an active alignment by optimizing the power read on the power meter. Some splicers can align the core of the fibers from the side view of the splicer camera; however, since the cladding of the Yb fiber has typically a shape such as octagonal to get rid of skew rays, this functionality is not very efficient to align the cores.

In theory, if the undoped fiber and Yb fiber have been designed to get a perfect match between their fundamental modes, a standard splice recipe should give good splice results; nevertheless, some mode mismatch always exists in practice. Adequate dopant diffusion<sup>[23],[24]</sup> during the splice process can help minimizing the splice loss and improving the transmission of the fundamental mode. From our experience, dopant diffusion improves the splice and gives lower splice loss than predicted by the theory of direct butt coupling for high NA fibers. Different parameters of the splice program can be modified such as the arc time, arc power, arc position, etc. A very clear example of the dopant diffusion is shown on Figure 10. The splice loss as a function of arc time is shown between a Corning HI1060 fiber (around  $5\mu\text{m}/0.14\text{NA}$ ) and a  $15\mu\text{m}/0.13\text{NA}$  Yb fiber. The Yb fiber is inserted between to HI1060 as shown on Figure 9 such that the splice loss of the fundamental mode is measured. The theoretical splice loss should be around 1.0 dB as calculated by equations 2 but the measured splice loss is around 0.58 dB. By further increasing the arc time to 16 s the splice loss decreases to 0.37 dB. This was achieved using a standard telecommunication splicer (Fitel S175).

It can be noted that a CCD camera was also tried to optimize the fundamental mode coupling through output mode profile measurement but we found out that it was less effective than the above described method to improve the fundamental mode transmission.

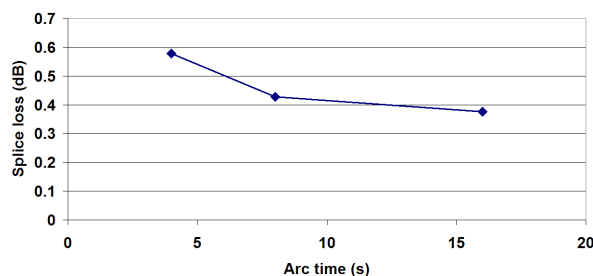


Figure 10. Splice loss of LP01 mode as a function of arc power when splicing a HI1060 fiber ( $\sim 5\mu\text{m}/0.14\text{NA}$ ) to a  $15\mu\text{m}/0.13\text{NA}$  fiber. The splice loss is way below the predicted theoretical value of 1.0 dB and a longer arc further decreases the splice loss.

## 4.2 Amplifier and laser tests

The proposed configuration of using high NA MM Yb fiber to obtain singlemode output was tested using different fiber design. In each case, the ytterbium fiber was spliced to the undoped SM fibers using the above described splice method. The fastest way to test a configuration is to do an amplifier setup since no FBG has to be written in the undoped fibers used. A typical amplifier results is shown on Figure 11. A  $10\mu\text{m}/0.20\text{NA}$  Yb high NA MM with  $125\mu\text{m}$  octagonal cladding is tested in an amplifier configuration. A 200 mW signal at 1064 nm is injected with a 6+1->1 combiner with a signal feedthrough and the fiber is co-pumped with 25 W of pump power at 915 nm. The fiber has 2.8 dB/m of cladding

absorption at 915 nm and a length of 4 m is used to get a total pump absorption between 10 to 15 dB which is typically optimum.

The slope efficiency of the fiber itself can be measured using a MM undoped fiber as the input and output to inject and gather the signal in all modes. In this case, a slope efficiency of 65% was measured. Then, the MM fiber is replaced by a singlemode fiber to test the efficiency of the system in singlemode operation. A 6 $\mu\text{m}/0.12\text{NA}$  and 5 $\mu\text{m}/0.14\text{NA}$  SM fiber were tested successively. Note that for all the mentioned case, single cladding undoped fibers were used at the output to get rid of all cladding mode and to measure only the signal power exiting the core. A lower slope efficiency was obtained when operating the MM fiber in singlemode operation: 59.6% slope efficiency was measured instead of 65.0 %, which corresponds to a slope efficiency loss of 5.4 % or an output power loss of 8.2% (59.6/65.0). This was expected from the theoretical analysis since coupling to higher order modes occur at the input splice from the SM fiber to the MM fiber and these modes are filtered out at the output splice when going back into the SM fiber. The SM 5 $\mu\text{m}/0.14\text{NA}$  gives lower slope efficiency than the 6 $\mu\text{m}/0.12\text{NA}$  due to the greater fundamental mode mismatch with the Yb MM fiber. The same Yb fiber was also tested in laser operation with FBG written in 6 $\mu\text{m}/0.12\text{NA}$  fiber and similar slope efficiencies were obtained than in amplifier configuration when the output coupling loss of the low reflectivity FBG is subtracted.

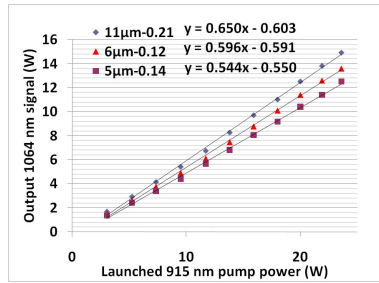


Figure 11. Slope efficiency of a 10 $\mu\text{m}/0.20\text{NA}$  high NA MM Yb fiber operated in amplifier configuration for different single cladding optical fiber used as the relay fiber.

Different MM high NA ytterbium fibers were tested in a similar manner. The test results are summarized in Table 1 along with the passive splice loss measurement at 1310 nm. The calculated V-number is also tabulated and shows that there is a limitation in the number of higher order modes supported by the MM fiber to get efficient singlemode operation. A significant efficiency loss was measured when using the highly MM 13 $\mu\text{m}/0.20\text{NA}$  Yb fiber and almost no efficiency loss happened with the slightly MM 7 $\mu\text{m}/0.18\text{NA}$  Yb fiber. This was observed on both the passive splice loss measurement and the amplifier test; a slight loss difference occurs between the passive test at 1310 nm and the active test at 1064 nm because a different number of modes are supported and a difference in MFD occurs between these two operation wavelengths.

There is therefore an upper limit in the number of supported modes by the MM Yb fiber to ensure an efficient singlemode operation using multimode fibers. For most cases with V-number up to values of 7.0, high NA MM fiber can operate in singlemode operation with slope efficiency losses of less than 5% compared to the intrinsic efficiency of the fiber itself. This efficiency reduction of 5% can be easily compensated by pump high NA MM phosphosilicate fiber at 965 nm instead of 915 nm due to the reduction of quantum defect as explained in section 2.4. It can be noted that the multimode efficiency of ytterbium is typically more in the 70-80% range but several of the ytterbium fibers used in table 1 were not optimized for low background losses and high efficiency; the goal was only to validate that multimode fibers can be operated in the fundamental mode with low loss in slope efficiency.

Ytterbium fiber (OD / NA)	Undoped fiber (OD / NA)	V-number	Supported higher order LP <sub>0x</sub> modes	Multimode slope efficiency (%)	Slope efficiency loss from MM to SM operation (%)	Passive splice loss at 1310 nm (%)
7 $\mu\text{m}$ / 0.18	5 $\mu\text{m}$ / 0.14	3.8	None	55	0.5	0.8
11 $\mu\text{m}$ / 0.18	6 $\mu\text{m}$ / 0.12	5.8	LP <sub>02</sub>	66	3	2.2
10 $\mu\text{m}$ / 0.20	6 $\mu\text{m}$ / 0.12	5.8	LP <sub>02</sub>	65	5	1.9
15 $\mu\text{m}$ / 0.13	8 $\mu\text{m}$ / 0.10	5.7	LP <sub>02</sub>	65	4	2.3
13 $\mu\text{m}$ / 0.20	8 $\mu\text{m}$ / 0.10	7.7	LP <sub>02</sub> , LP <sub>03</sub>	76	13	7.0

Table 1. Efficiency tests in amplifier configuration of different ytterbium fiber with their corresponding singlemode undoped fiber used. The multimode slope efficiency is shown with respect to the absorbed pump power at 915 nm.

It can be noted that the best matching undoped singlemode fiber for the 15 $\mu\text{m}/0.13\text{NA}$  Yb fiber could be a 10 $\mu\text{m}/0.08\text{NA}$  because of the MFD match. Nevertheless, it was measured that a higher efficiency is obtained with an 8 $\mu\text{m}/0.10\text{NA}$  singlemode undoped fiber even if the MFD mismatch is larger. We believe that this is caused by the dopant diffusion during the splice process of low NA fibers. Any refractive index perturbation can easily affect the propagating mode in low NA regime as shown on Figure 2 in section 2.2. Therefore in some design, it might be appropriate to use slightly multimode undoped fiber, such as a 10 $\mu\text{m}/0.10\text{NA}$  to match the high NA MM Yb fiber and still preserves fundamental mode operation. The first HOM, the LP<sub>11</sub>, would not be significantly excited in the undoped fiber.

### 4.3 High power demonstration

The MM design was tested at high power in both a master oscillator (MO) and a power amplifier (PA) using the configurations shown on Figure 1. The fiber laser was made with an Yb MM high NA fiber of 10 $\mu\text{m}/0.20\text{NA}$  with FBG written in 6 $\mu\text{m}/0.12\text{NA}$  singlemode fiber and the power amplifier was done with a 15 $\mu\text{m}/0.13\text{NA}$  Yb fiber pigtailed with 8 $\mu\text{m}/0.10\text{NA}$  undoped fiber. Both fibers had 125  $\mu\text{m}$  cladding diameter. As demonstrated in section 2.3, the mode area of the 15 $\mu\text{m}/0.13\text{NA}$  fiber of the power amplifier should allow operation up to the kW level without stimulated Raman scattering. Both stages have an overall system slope efficiency of 50% where the MO give 45W of output power and the power amplifier further amplified the signal to 75W. The power was mainly limited by the pump power that could be efficiently injected in the 125  $\mu\text{m}$  cladding fiber from the available components used. The overall system efficiency was lowered than the intrinsic fiber efficiency shown previously due to cladding losses of the FBGs and combiners.

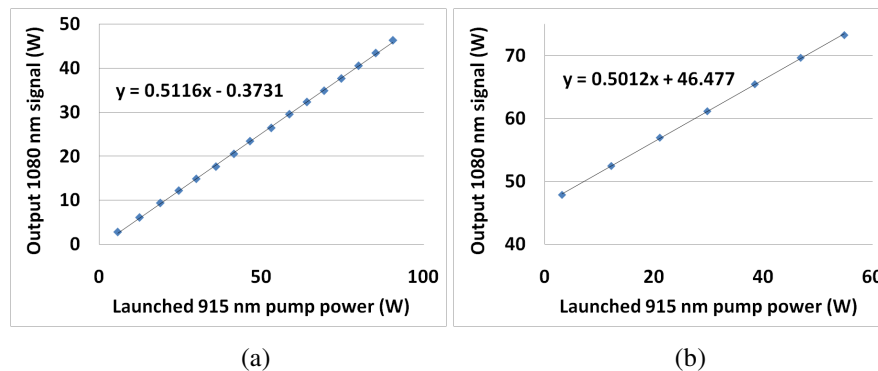


Figure 12. Slope efficiency with respect to the launched pump power at 915 nm of (a) a master oscillator made with 10 $\mu\text{m}/0.20\text{NA}$  Yb fiber spliced to FBGs made in 6 $\mu\text{m}/0.12\text{NA}$  and (b) a power amplifier made with 15 $\mu\text{m}/0.13\text{NA}$  Yb fiber pigtailed with 8 $\mu\text{m}/0.10\text{NA}$  undoped fiber.

## 5. CONCLUSION

The use of multimode high NA fiber was thoroughly investigated to achieve high power CW fiber laser and amplifier operating in the fundamental mode. Motivations of such design over more conventional LMA low NA fibers were presented such as the large tolerances of high NA fibers in term of mode field stability, spliceability and the capability to easily write FBGs with standard UV inscription method. It was also shown that a small mode field diameter of 11  $\mu\text{m}$  obtained in high NA fiber is enough to reach the kW level in most amplifier configurations with 25 m of fiber length. Furthermore, high photodarkening mitigation and more efficient 960 nm pumping are described with phosphorous codoping that can easily be incorporated with high NA fiber. The theoretical analysis of such design was done where the mode field matching was optimized between the singlemode fiber and the high NA multimode fiber from a simple analytical model or more complete stratified modelisation of the refractive index profile. Minimizing higher order mode excitation was also discussed by selecting the proper V-number to limit the total number of modes and obtain a large enough modal index difference to avoid intermodal coupling. Appropriate splice optimization was presented to compensate for slight MFD mismatch and optimize fundamental mode operation. Several tests in amplifier and laser configuration were conducted with different MM high NA fiber configuration. The singlemode operation typically brought less than 5% loss in slope efficiency compared to the multimode efficiency for V-number up to a value of 7.0 and a high power 75 W output power was demonstrated using a MOPA configuration.

## REFERENCES

- [1] Gapontsev, D., "6 kW CW single mode ytterbium fiber laser in all-fiber format," Conf. on Solid State and Diode Laser Tech. Review, Directed Energy Professional Society, Albuquerque, New Mexico (2008).
- [2] Agrawal, G.P., [Nonlinear Fiber Optics], Academic Press, San Diego, (2001).
- [3] Liu, C.-H., Galvanauskas, A., Ehlers, B., Doerfel, F., Heinemann, S., Carter, A., Tanakala, K., Farroni, J., "700-W single transverse mode Yb-doped fiber laser," Conf. on Laser and Elec.-Opt., (2004).
- [4] Jeong, Y., Sahu, J. K., Payne, D. N., Nilsson, J., "Ytterbium-doped large-core fiber laser with 1.36 kW continuous-wave output power," Opt. Exp. 12 (25), 6088-6092 (2004).
- [5] Koplrow, J. P., Kliner, D. A. V., Goldberg, L., "Single-mode operation of a coiled multimode fiber amplifier," Opt. Lett. 25 (7), 442-444 (2000).
- [6] Wirth, C., Schmidt, O., Tsybin, I., Schreiber, T., Limpert, J., Eberhardt, R., Tünnermann, A., "1 kW narrow-linewidth fiber amplifier for spectral beam combining," Adv. Solid-State Phot., WA6 (2008).
- [7] Alvarez-Chavez, J. A., Grudinin, A. B., Nilsson, J., Turner, P. W., Clarkson, W. A., "Mode Selection in high power cladding pumped fiber lasers with tapered section," Conf. on Lasers and Electro-Opt., CWE7 (1999).
- [8] Faucher, M., Keith Lize, Y., "Mode Field Adaptation for High Power Fiber Lasers," Conf. on Lasers and Electro-Opt. CF17, (2007).
- [9] Fermann, M. E., "Single-mode excitation of multimode fibers with ultrashort pulses," Opt. Lett. 23 (1), 52-54 (1998).
- [10] Fermann, M. E., Galvanauskas, A., Harter, D., Minelly, J.D., Caplen, J.E., "High-power singlemode fiber amplifiers using multimode fibers," Opt. Fib. Comm. Conf., TuG8 (1998).
- [11] Sévigny, B., Zhang, X., Garneau, M., Faucher, M., Keith Lizé, Y., Holehouse, N., "Modal sensitivity analysis for single mode operation in large mode area fiber," Proc. SPIE 6873, 68730A (2008).
- [12] Morasse, B., Chatigny, S., Gagnon, E., de Sando, J.-P., Desrosiers, C., "Enhanced Pulseshaping Capabilities and Reduction of Non-Linear Effects in All-fiber MOPA Pulsed System," Proc. SPIE 7195, 7195-48 (2009).
- [13] Koponen, J. J. Söderlund, M. J., Hoffman, H. J., Tammela, S. K. T., "Measuring photodarkening from single-mode ytterbium doped silica fibers," Opt. Expr. 14 (24), 11539-11544 (2006).
- [14] Morasse, B., Chatigny, S., Gagnon, E., Hovington, C., Martin, J.-P., de Sandro, J.-P., "Low photodarkening single cladding ytterbium fibre amplifier," Proc. SPIE 6453, 64530H (2007).
- [15] Jetschke, S., Unger, S., Schwuchow, A., Leich, M., Kirchhof, J., "Efficient Yb laser fibers with low photodarkening by optimization of the core composition," Opt. Expr. 16 (20), 15540-15545 (2008).
- [16] Lee, Y.W., Sinha, S., Digonnet, M. J. F., Byer, R. L., Jiang, S., "Measurement of high photodarkening resistance in heavily yb31-doped phosphate fibres," Elec. Lett. 44 (1), 14-16 (2008).
- [17] Engholm, M., Norin, L., "Preventing photodarkening in ytterbium-doped high power fiber lasers; correlation to the UV-transparency of the core glass," Opt. Expr. 16 (2), 1260-1268 (2008).
- [18] Sahu, J. K., Yoo, S., Boyland, A. J., Basu, C., Kalita, M. P. Webb, A., Sones, C. L., Nilsson, J., Payne, D. N., "488 nm irradiation induced photodarkening study of Ybdoped aluminosilicate and phosphosilicate fibers," Proc. of CLEO/QELS, JTuA27 (2008).
- [19] Senior, J. M., [Optical Fiber Communications, Principles and Practice 2<sup>nd</sup> ed.], Prentice Hall International, Hertfordshire, United Kingdom, (2008).
- [20] Buck, J. A., [Fundamentals of Optical Fibers], Wiley, New-York, (1995).
- [21] Yeh C., Lindgren, G., "Computing the propagation characteristics of radially stratified fibers: an efficient method," Appl. Opt. 16, 483-493 (1977).
- [22] Laperle, P., Paré, C., Zheng, H., Croteau, A., "Yb-Doped LMA Triple-Clad Fiber for Power Amplifiers," Proc. SPIE 6453, 6453-08 (2007).
- [23] Kihara, M., Matsumoto, M., Haibara, T., Tomita, S. "Characteristics of Thermally Expanded Core Fiber," Jour. Light. Tech. 14 (10), 2209-2214 (1996).
- [24] Kato, K., Nishi, I., Yoshino, K., Hanafusa, H. "Optical coupling characteristics of laser diodes to thermally diffused expanded core fiber using an aspheric lens," IEEE Phot. Tech. Lett. 3, 469-470 (1991).